
Attention Solves Your TSP

W. W. M. Kool^{1,2} M. Welling¹

Abstract

We propose a framework for solving combinatorial optimization problems of which the output can be represented as a sequence of input elements. As an alternative to the Pointer Network, we parameterize a policy by a model based entirely on (graph) attention layers, and train it efficiently using REINFORCE with a simple and robust baseline based on a deterministic (greedy) rollout of the best policy found during training. We significantly improve over state-of-the-art results for learning algorithms for the 2D Euclidean TSP, reducing the optimality gap for a single tour construction by more than 75% (to 0.33%) and 50% (to 2.28%) for instances with 20 and 50 nodes respectively.

1. Introduction

Imagine yourself traveling to a scientific conference. The field is popular, there is a lot of research and you are on a tight schedule to make sure you do not miss out on anything. You carefully selected n posters that you want to see, but in order to have time to actually study them, it is important that you minimize your time walking around. Naturally, after visiting all n posters, you want to return to the place you are now: the coffee corner. The problem is: in which order should you visit the posters? Let us call this problem the Travelling Scientist Problem (TSP).

You realize that your problem is mathematically equivalent to the Travelling Salesman Problem (conveniently also abbreviated as TSP). This seems discouraging as you know people have studied the problem and it is hard, or from the perspective of complexity theory, NP-hard (Garey & Johnson, 1979). Fortunately, complexity theory analyzes the worst-case scenario, and your Bayesian view of the world does not consider the worst case very likely. In particular, you have a strong prior: the organization will probably lay out the locations regularly over the available space. Therefore, you would be happy with a specialized algorithm that

solves not any, but *this* type of problem instance well. You have some months left and to not waste any time, you want to prepare your algorithm upfront. Given recent successes in machine learning, you wonder whether your algorithm can be learned?

1.1. Motivation

Machine learning algorithms have replaced humans as the engineers of algorithms to solve various tasks. A decade ago, computer vision algorithms used hand-crafted features but today they are learned *end-to-end* by Deep Neural Networks (DNNs). DNNs have outperformed classic approaches to speech recognition, machine translation, image captioning and many other problems, by learning from data (LeCun et al., 2015). While DNNs are mainly used to make *predictions*, Reinforcement Learning (RL) has enabled algorithms to learn to make *decisions*, either by interaction with an environment to learn to play Atari games (Mnih et al., 2015), or by inducing knowledge through look-ahead search: this was used to master the game of Go (Silver et al., 2017).

The world is not a game, and we desire to train models that can make decisions to solve real problems. These must be able to learn to select good solutions for a problem from a combinatorially large set of potential solutions. Classically, approaches to this problem of *combinatorial optimization* can be divided into *exact methods*, that guarantee finding optimal solutions, and *heuristics*, that trade off optimality for computational cost, although exact methods can use heuristics internally and vice versa. Heuristics are typically expressed in the form of rules, which can be interpreted as policies to make decisions. We believe that these policies can be parameterized using DNNs, and be trained to obtain stronger algorithms for combinatorial optimization problems, similar to the way DNNs have boosted performance in the applications mentioned before.

1.2. Attention model for combinatorial optimization

In this paper, we take a step forward towards our goal of learning algorithms for combinatorial optimization problems. We parameterize a stochastic policy by a model based on (graph) attention layers, which can construct a solution by outputting input elements as a sequence. We show how to efficiently train this model using REINFORCE (Williams,

¹University of Amsterdam, The Netherlands ²ORTEC Optimization Technology, The Netherlands. Correspondence to: W.W.M. Kool <w.w.m.kool@uva.nl>.

1992) with a simple and robust baseline based on a deterministic (greedy) rollout of the best policy found during training so far. We focus on the 2D Euclidean TSP as a classical example of a combinatorial optimization problem and significantly improve over state-of-the-art results of learned algorithms for this problem.

Attention model Our model consists of an encoder and a decoder, both entirely based on attention. The encoder uses a stack of multi-head attention layers (Vaswani et al., 2017) to compute embeddings of all nodes in the instance, while the decoder uses a single layer of multi-head attention over the input and a (single-head) attention mechanism to define a probability distribution over the input nodes. The overall model is very similar to the Transformer architecture by Vaswani et al. (2017) but does not have a fixed output vocabulary. Since the layers in the model are effectively attention-based graph convolutions (Veličković et al., 2017), the model is readily applicable to general graphs, therefore generalizable to other combinatorial optimization problems. The model is autoregressive, and computes the next node to output based on context from previous output, but does *not* have a recurrent state. We believe this is appropriate as the state in an optimization problem is fully observable.¹

REINFORCE with rollout baseline We train our model using REINFORCE by rolling out the computational graph of the auto-regressive model and backpropagating through it to update the policy, based on a Monte Carlo estimate of the loss (the cost/tour length of the solution). By using as baseline a deterministic rollout of the best policy seen during training, we encourage the policy to improve over itself, similar to the self-play improvement scheme used by Silver et al. (2017).

2. Related work

The application of Neural Networks (NNs) for optimizing decisions in combinatorial optimization problems dates back to Hopfield & Tank (1985), who applied a Hopfield-network for solving small TSP instances. NNs have been applied to many related problems (Smith, 1999), although in most cases as a computation model in an *online* manner, starting ‘from scratch’ and ‘learning’ a solution for every instance. More recently, (D)NNs have also been used in an *offline* manner to learn about a class of problem instances rather than a single one.

¹We think that theoretically there can be a computational advantage by having a recurrent state, since the model can learn to re-use/pass forward computation to subsequent steps. However, empirically we find that a global recurrent state can be omitted for the TSP problem without loss in accuracy.

Vinyals et al. (2015b) introduce the Pointer Network (PN) as a model that uses attention to output a permutation of the input, and train this model offline to solve the (Euclidean) TSP, supervised by example solutions. Upon test time, they apply a beam search procedure that filters invalid tours. Bello et al. (2016) note that supervised solutions are not always available and introduce an Actor-Critic algorithm to train the PN. Similar to Vinyals et al. (2015b) they consider each instance as a training sample and use the cost (tour length) of a sampled solution for an unbiased Monte-Carlo estimate of the policy gradient. They introduce extra model depth in the decoder by an additional *glimpse* (Vinyals et al., 2015a) at the embeddings, masking nodes already visited. For small instances ($n = 20$), they get close to the results by Vinyals et al. (2015b) and improve for $n = 50$ by also training for $n = 50$ (the original PN was trained only on up to 20 nodes).

Dai et al. (2017) do not use a separate encoder and decoder, but a single model based on graph embeddings. They train the model to output the *order* in which nodes are *inserted* into a partial tour, using a helper function to insert at the best possible location. Their DQN (Mnih et al., 2015) training method with $n = 1$ trains the algorithm per step and incremental rewards provided to the agent at every step effectively encourage greedy behavior. Additionally, they flip the reward², which combined with discounting encourages the agent to insert the farthest nodes first, which is known to be an effective heuristic (Rosenkrantz et al., 2009).

Nowak et al. (2017) train a Graph Neural Network in a supervised manner to directly output the optimal tour in the form of an adjacency matrix which is converted into a feasible solution by a beam search. The model is non-autoregressive, so cannot condition its output on the partial tour and the authors report an optimality gap of 2.7% for $n = 20$, worse than autoregressive approaches.

Finally, we note that all of the mentioned papers have not included as a baseline the farthest insertion heuristic, a simple algorithm that greedily inserts the most distant node into the tour at the best possible location and is known empirically to outperform nearest or random order insertion (Rosenkrantz et al., 2009). We show that we can consistently outperform this baseline and the approaches mentioned here in Section 6.

3. Attention model

We define a problem instance s as a graph with n nodes, where node $i \in \{1, \dots, n\}$ is represented by features \mathbf{x}_i . In

²The authors mention flipping of the reward in the appendix on <https://papers.nips.cc/paper/7214-learning-combinatorial-optimization-algorithms-over.zip>.

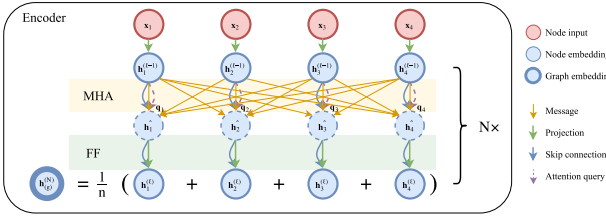


Figure 1. Attention based encoder. Input nodes are embedded and processed by N sequential layers, each consisting of a multi-head attention (MHA) and node-wise feed-forward (FF) sublayer. The embedding of the graph is computed as the mean of all node embeddings. Best viewed in color.

our implementation for TSP, the graph is fully connected (including self-connections) and \mathbf{x}_i is the (x, y) coordinate of node i . We define a solution (tour) π as a permutation of the nodes, e.g. $\pi = (\pi_1, \dots, \pi_n)$ with $\pi_t \in \{1, \dots, n\}$ and $\pi_t \neq \pi_{t'} \forall t \neq t'$. Our attention based encoder-decoder model defines a stochastic policy $p(\pi|s)$ for selecting a solution π given a problem instance s . It is factorized and parameterized by θ as

$$p(\pi|s) = \prod_{t=1}^n p_{\theta}(\pi_t|s, \pi_{1:t-1}). \quad (1)$$

The encoder produces embeddings of all input nodes. The decoder produces the sequence π of input nodes, one node at a time. It takes as input the embeddings from the encoder and, being autoregressive, a context based on the partial solution constructed so far. For the TSP, the context consists of the graph embedding, the previous node that was selected (similar to the Pointer Network) and the first node as this is relevant information (the tour should end here) which cannot be used by the model otherwise.

3.1. Encoder

The encoder that we use (Figure 1) is similar to the encoder used in the Transformer architecture (Vaswani et al., 2017), but we do not use positional encoding such that the resulting node embeddings are invariant to the input order. From the d_x -dimensional input features \mathbf{x}_i (for TSP $d_x = 2$), the encoder computes initial d_h -dimensional node embeddings $\mathbf{h}_i^{(0)}$ (we use $d_h = 128$) through a learned linear projection with parameters W^x and b^x :

$$\mathbf{h}_i^{(0)} = W^x \mathbf{x}_i + b^x. \quad (2)$$

The embeddings are updated using $N = 3$ attention layers, each consisting of two sublayers. We denote with $\mathbf{h}_i^{(\ell)}$ the node embeddings produced by layer $\ell \in \{1, \dots, N\}$. The encoder computes an aggregated embedding $\mathbf{h}_g^{(N)}$ of the

input graph as the mean of the final node embeddings $\mathbf{h}_i^{(N)}$:

$$\mathbf{h}_g^{(N)} = \frac{1}{n} \sum_{i=1}^n \mathbf{h}_i^{(N)}. \quad (3)$$

Both the node embeddings $\mathbf{h}_i^{(N)}$ and the graph embedding $\mathbf{h}_g^{(N)}$ are used as input to the decoder.

Attention layer Following the architecture by Vaswani et al. (2017), each attention layer consists of two sublayers: a multi-head attention (MHA) layer that executes message passing between the nodes and an node-wise fully connected feed-forward (FF) layer. Each sublayer adds a skip-connection (He et al., 2016) and batch normalization³ (BN) (Ioffe & Szegedy, 2015):

$$\hat{\mathbf{h}}_i = \text{BN}^{\ell} \left(\mathbf{h}_i^{(\ell-1)} + \text{MHA}_i^{\ell} \left(\mathbf{h}_1^{(\ell-1)}, \dots, \mathbf{h}_n^{(\ell-1)} \right) \right) \quad (4)$$

$$\mathbf{h}_i^{(\ell)} = \text{BN}^{\ell} \left(\hat{\mathbf{h}}_i + \text{FF}^{\ell}(\hat{\mathbf{h}}_i) \right). \quad (5)$$

We superscript BN, FF and MHA with the layer index ℓ to indicate that the layers do *not* share parameters.

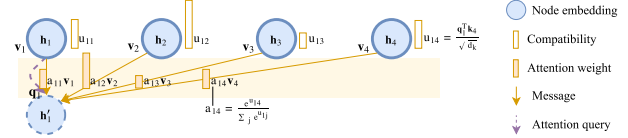


Figure 2. Illustration of weighted message passing using a dot-attention mechanism. Only computation of messages received by node 1 are shown for clarity. Best viewed in color.

Attention mechanism We interpret the attention mechanism (in Equation (4)) by Vaswani et al. (2017) as a weighted message passing algorithm between nodes in a graph. The weight of the message *value* that a node receives from a neighbor depends on the *compatibility* of its *query* with the *key* of the neighbor, as illustrated in Figure 2. Formally, we define dimensions d_k and d_v and compute the key $\mathbf{k}_i \in \mathbb{R}^{d_k}$, value $\mathbf{v}_i \in \mathbb{R}^{d_v}$ and query $\mathbf{q}_i \in \mathbb{R}^{d_k}$ for each node by projecting the embedding \mathbf{h}_i :

$$\mathbf{q}_i = W^Q \mathbf{h}_i, \quad \mathbf{k}_i = W^K \mathbf{h}_i, \quad \mathbf{v}_i = W^V \mathbf{h}_i. \quad (6)$$

Here parameters W^Q and W^K are $(d_k \times d_h)$ matrices and W^V has size $(d_v \times d_h)$. From the queries and keys, we compute the compatibility $u_{ij} \in \mathbb{R}$ of the query \mathbf{q}_i of node

³We found batch normalization to work better than layer normalization, as used by Vaswani et al. (2017).

i with the key \mathbf{k}_j of node j as the (normalized, see Vaswani et al. (2017)) dot-product:

$$u_{ij} = \begin{cases} \frac{\mathbf{q}_i^T \mathbf{k}_j}{\sqrt{d_k}} & \text{if } i \text{ adjacent to } j \\ -\infty & \text{otherwise.} \end{cases} \quad (7)$$

In a general graph, defining the compatibility of non-adjacent nodes as $-\infty$ prevents message passing between these nodes. From the compatibilities u_{ij} , we compute the *attention weights* $a_{ij} \in [0, 1]$ using a softmax:

$$a_{ij} = \frac{e^{u_{ij}}}{\sum_{j'} e^{u_{ij'}}}. \quad (8)$$

Finally, the vector \mathbf{h}'_i that is received by node i is the convex combination of messages \mathbf{v}_j :

$$\mathbf{h}'_i = \sum_j a_{ij} \mathbf{v}_j. \quad (9)$$

Multi-head attention As was noted by Vaswani et al. (2017) and (Veličković et al., 2017), it is beneficial to have multiple attention heads. This allows nodes to receive different types of messages from different neighbors. Especially, we compute the value (9) $M = 8$ times with different parameters, using $d_k = d_v = \frac{d_h}{M} = 16$. We denote the result vectors by \mathbf{h}'_{im} for $m \in 1, \dots, M$. These are projected back to a single d_h -dimensional vector using $(d_h \times d_v)$ parameter matrices W_m^O . The final multi-head attention value for node i is a function of $\mathbf{h}_1, \dots, \mathbf{h}_n$ through \mathbf{h}'_{im} :

$$\text{MHA}_i(\mathbf{h}_1, \dots, \mathbf{h}_n) = \sum_{m=1}^M W_m^O \mathbf{h}'_{im}. \quad (10)$$

Feed-forward sublayer The feed-forward sublayer (in Equation (5)) computes node-wise projections using a hidden (sub)sublayer with dimension $d_{ff} = 512$ and a ReLu activation:

$$\text{FF}(\mathbf{h}_i) = W^{\text{ff},1} \cdot \text{ReLU}(W^{\text{ff},0} \mathbf{h}_i + \mathbf{b}^{\text{ff},0}) + \mathbf{b}^{\text{ff},1}. \quad (11)$$

Batch normalization We use batch normalization with learnable d_h -dimensional affine parameters \mathbf{w}^{bn} and \mathbf{b}^{bn} :

$$\text{BN}(\mathbf{h}_i) = \mathbf{w}^{\text{bn}} \odot \overline{\text{BN}}(\mathbf{h}_i) + \mathbf{b}^{\text{bn}}. \quad (12)$$

Here \odot denotes the element-wise product and $\overline{\text{BN}}$ refers to batch normalization without affine transformation. We found that it is important to initialize the parameters small enough, e.g. uniform within $(-\frac{1}{\sqrt{d_h}}, \frac{1}{\sqrt{d_h}})$.

3.2. Decoder

Decoding happens sequentially, and at timestep $t \in \{1, \dots, n\}$, the decoder outputs the node π_t based on the

embeddings from the encoder and the outputs $\pi_{t'}$ generated at time $t' < t$. During decoding, we augment the graph with a special *context node* (c) to represent the decoding context. The decoder computes an attention (sub)layer on top of the encoder, but with messages only to the context node for efficiency.⁴ The final probabilities are computed using a single-head attention mechanism. See Figure 3 for an illustration of the decoding process.

Context embedding The context of the decoder at time t comes from the encoder and the output up to time t . As explained, for the TSP it consists of the embedding of the graph, the previous (last) node π_{t-1} and the first node π_1 . For $t = 1$ we use learned d_h -dimensional input symbols \mathbf{v}^l and \mathbf{v}^f :

$$\mathbf{h}_{(c)}^{(N)} = \begin{cases} [\mathbf{h}_{(g)}^{(N)}, \mathbf{h}_{\pi_{t-1}}^{(N)}, \mathbf{h}_{\pi_1}^{(N)}] & t > 1 \\ [\mathbf{h}_{(g)}^{(N)}, \mathbf{v}^l, \mathbf{v}^f] & t = 1. \end{cases} \quad (13)$$

Here $[\cdot, \cdot, \cdot]$ is the horizontal concatenation operator and we write the $(3 \cdot d_h)$ -dimensional result vector as $\mathbf{h}_{(c)}^{(N)}$ to indicate we interpret it as the embedding of the special context node (c) and use the superscript (N) to align with the node embeddings $\mathbf{h}_i^{(N)}$. We could project the embedding back to d_h dimensions, but we absorb this transformation in the parameter W^Q in Equation (14).

Now we compute a new context node embedding $\mathbf{h}_{(c)}^{(N+1)}$ using the (M -head) attention mechanism described in Section 3.1. The keys and values come from the node embeddings $\mathbf{h}_i^{(N)}$, but we only compute a single query $\mathbf{q}_{(c)}$ (per head) from the context node (we omit the (N) for readability):

$$\mathbf{q}_{(c)} = W^Q \mathbf{h}_{(c)} \quad \mathbf{k}_i = W^K \mathbf{h}_i, \quad \mathbf{v}_i = W^V \mathbf{h}_i. \quad (14)$$

We compute the compatibility of the query with all nodes, where we mask the nodes that are already in the output:

$$u_{(c)j} = \begin{cases} \frac{\mathbf{q}_{(c)}^T \mathbf{k}_j}{\sqrt{d_k}} & \text{if } j \neq \pi_{t'} \quad \forall t' < t \\ -\infty & \text{otherwise.} \end{cases} \quad (15)$$

Again, we compute $u_{(c)j}$ and \mathbf{v}_i for $M = 8$ heads and compute the final multi-head attention value for the context node using Equations (8), (9) and (10), but with (c) instead of i . The result $\mathbf{h}_{(c)}^{(N+1)}$ is similar to the *glimpse* value described by Bello et al. (2016), but unifies with our model using multi-head attention. Note that we do *not* add skip-connections, batch normalization and the feed-forward sublayer in the decoder. We did not experiment with using more than one layer to update the context in the decoder.

⁴ $n \times n$ attention between all nodes is expensive to compute in every step of the decoding process.

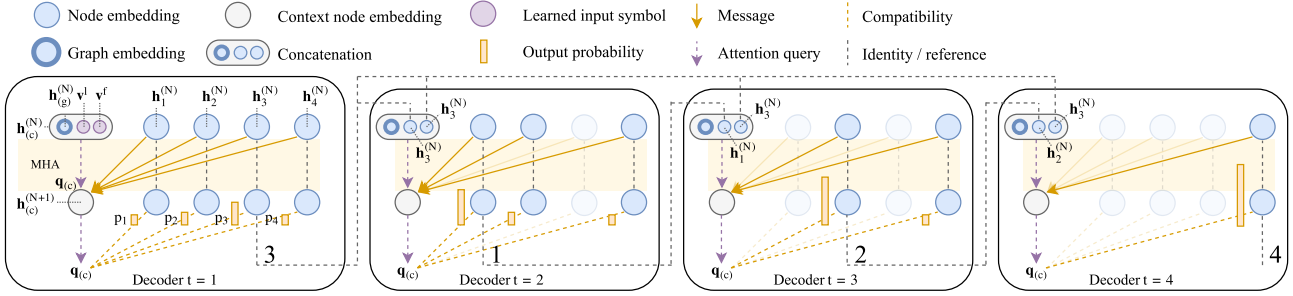


Figure 3. Attention based decoder for the TSP problem. The decoder takes as input the graph embedding and node embeddings. At each time step t , the context consist of the graph embedding and the embeddings of the first and last (previously output) node of the partial tour, where learned input symbols are used if $t = 1$. Nodes already in the output are masked. The example shows how a tour $\pi = (3, 1, 2, 4)$ is constructed. Best viewed in color.

Calculation of log-probabilities In order for the model to compute output probabilities $p_\theta(\pi_t|s, \pi_{1:t-1})$ in Equation (1), we add one final decoder layer with a *single* attention head, for which we only compute the compatibilities $u_{(c)j}$ using Equation (15), but following Bello et al. (2016) we clip the result (before masking!) within $[-C, C]$ ($C = 10$) using a tanh:

$$u_{(c)j} = \begin{cases} C \cdot \tanh\left(\frac{\mathbf{q}_{(c)}^T \mathbf{k}_j}{\sqrt{d_k}}\right) & \text{if } j \neq \pi_t \quad \forall t < t' \\ -\infty & \text{otherwise.} \end{cases} \quad (16)$$

We interpret these compatibilities as unnormalized log-probabilities (logits) and compute the final output probability vector \mathbf{p} using a softmax (similar to Equation (8)):

$$p_i = p_\theta(\pi_t = i|s, \pi_{1:t-1}) = \frac{e^{u_{(c)i}}}{\sum_j e^{u_{(c)j}}}. \quad (17)$$

4. REINFORCE with rollout baseline

In Section 3 we defined our model that given an instance s defines a probability distribution $p_\theta(\pi|s)$, which we can sample from to obtain solutions (tours) $\pi|s$. In order to train our model, we define a loss \mathcal{L} based on the cost (length of the tour) $L(\pi)$ that we can optimize with respect to the parameters θ :

$$\mathcal{L}(\theta|s) = \mathbb{E}_{p_\theta(\pi|s)}(L(\pi)). \quad (18)$$

We optimize (18) by gradient descent, using the REINFORCE (Williams, 1992) estimator with baseline $b(s)$:

$$\nabla \mathcal{L}(\theta|s) = \mathbb{E}_{p_\theta(\pi|s)}((L(\pi) - b(s)) \nabla \log p_\theta(\pi|s)). \quad (19)$$

Using a good baseline $b(s)$ reduces the variance of the estimator and increases the speed of learning.

4.1. Choice of baseline

Exponential Moving Average An exponential (moving average) baseline is simple to implement, fast to compute and accounts for the fact that \mathcal{L} decreases during training. In the first iteration, we set $M = L(\pi)$ after which every iteration it gets updated using a *decay* parameter β :

$$M \leftarrow \beta M + (1 - \beta)L(\pi). \quad (20)$$

The major drawback of the baseline function $b(s) = M$ is that it does not depend on s .

Critic When s is interpreted as the state in a Reinforcement Learning setting, a natural choice for the baseline is an estimate of the state-value function, also referred to as a *critic*, parameterized by w : $\hat{v}(s, w)$. A critic can differentiate between instances and thus potentially reduce variance more than the exponential moving average. In our case, \hat{v} can be learned from the observations $(s, L(\pi))$, which are Monte-Carlo estimates of the true value function. However, parameterization and learning of \hat{v} introduce additional hyperparameters and getting the algorithm to work well is non-trivial. When using the baseline $b(s) = \hat{v}(s, w)$, the value $L(\pi) - b(s)$ in (19) is an estimate of the advantage of the solution π .

4.2. Rollout as baseline

The rollout baseline that we propose is summarized as follows: define $b(s)$ to be the cost of a solution obtained by a deterministic (greedy) rollout of the algorithm defined by the best model so far.

Motivation The goal of a baseline is to predict the difficulty, or (negative) ‘value’, of the instance s , such that it can relate to the cost of the solution $L(\pi)$ to form an estimate of the advantage of the solution π selected by the model. We make an observation that is key to the baseline we propose:

The difficulty of an instance can (on average) be estimated by the performance of an (any!) algorithm applied to it.

This follows from the assumption that an algorithm will perform (in an absolute sense) worse on instances that are more difficult (have a higher optimal cost). This means that we can form a baseline simply by applying (rolling out) the algorithm defined by our model during training. For a stochastic policy, the result is of high variance, but we can easily enforce our policy to be deterministic by selecting the action with maximum probability (i.e. become greedy). As there is no stochasticity in the problem, this completely eliminates variance and thus defines a very stable baseline.

Determining the rollout policy As the model changes during training, we further stabilize the baseline by freezing the rollout policy for a fixed amount of steps (every epoch⁵), which can be regarded similar to freezing of the target Q-network in DQN (Mnih et al., 2015). Since a stronger algorithm defines a stronger baseline, we evaluate the current policy against the rollout policy at the end of every epoch, and replace the rollout policy only if the improvement is significant as determined by a paired t-test with $\alpha = 5\%$ on a separate (evaluation) dataset with 10000 instances. If the rollout policy is updated, we sample a new dataset to prevent overfitting.

Analysis Using the rollout policy as baseline $b(s)$, the function $L(\pi) - b(s)$ is negative if the sampled solution π improves over the greedy rollout solution, causing actions to be reinforced, and vice versa. Combined with the evaluation at the end of each epoch, this challenges the model to improve over itself, and we see strong similarities with the self-play improvement scheme that was successfully applied to master the game of Go (Silver et al., 2017).

Algorithm We use Adam (Kingma & Ba, 2014) as optimizer and summarize our REINFORCE training procedure with rollout baseline in Algorithm 1.

Efficiency Each rollout constitutes an additional forward pass, theoretically increasing computation by 50%. However, as the baseline policy is fixed for an epoch, we can sample the data and compute baselines per epoch using much larger batch sizes, allowed by the reduced memory requirement as the computations can run in pure inference mode. Empirically we find that it adds only 33%, taking up 25% of total computation. If desired, the baseline rollout can be easily parallelized on an additional GPU such that there is no increase in time per iteration.⁶

⁵The size of the epoch can be freely defined as instances are generated randomly.

⁶This is an easy way to benefit from an additional GPU, which is otherwise non-trivial because of the sequential model.

Algorithm 1 REINFORCE with Rollout Baseline

```

1: Input: number of epochs  $N$ , steps per epoch  $T$ , batch size  $B$ ,  

   significance  $\alpha$ 
2: Init  $\theta$ ,  $\theta^{BL} \leftarrow \theta$ 
3: for  $epoch = 1, \dots, N$  do
4:   for  $step = 1, \dots, T$  do
5:      $s_i \leftarrow \text{RandomInstance}() \quad \forall i \in \{1, \dots, B\}$ 
6:      $\pi_i \leftarrow \text{SampleRollout}(s_i, p_\theta) \quad \forall i \in \{1, \dots, B\}$ 
7:      $\pi_i^{BL} \leftarrow \text{GreedyRollout}(s_i, p_{\theta^{BL}}) \quad \forall i \in \{1, \dots, B\}$ 
8:      $\mathcal{L} \leftarrow \sum_{i=1}^B (L(\pi_i) - L(\pi_i^{BL})) \nabla_\theta \log p_\theta(\pi_i)$ 
9:      $\theta \leftarrow \text{Adam}(\theta, \mathcal{L})$ 
10:  end for
11:  if  $\text{OneSidedPairedTTest}(p_\theta, p_{\theta^{BL}}) < \alpha$  then
12:     $\theta^{BL} \leftarrow \theta$ 
13:  end if
14: end for

```

5. Experiments

We train separate models TSP20, TSP50 and TSP100 for TSP instances with 20, 50 and 100 nodes respectively. To show the benefit of our rollout baseline, we also run experiments using an exponential moving average baseline and a critic network for TSP20.

5.1. Training details

All parameters (weights and biases) are initialized uniformly within $(-\frac{1}{\sqrt{d}}, \frac{1}{\sqrt{d}})$, where d is the input dimension. We use a batch size of 512 with a learning rate of 10^{-3} and clip the gradient $L2$ norm to 1.0. Every epoch we process 1.28 million instances in 2500 iterations, after which we decay the learning rate by a factor 0.96. We run training for 100 epochs. Computing an epoch takes around 5 minutes for TSP20 and 16 for TSP50 on a single GPU (including baseline rollouts), while for TSP100 it takes 30 minutes on two GPUs.⁷

5.2. Evaluation

We evaluate our model in two different ways: using *greedy decoding* to always select the next node with maximum probability, and *sampling* to construct multiple solutions for a trade-off between quality of the solution and computation time. We evaluate our results on held-out test datasets with 10000 instances for each problem size n , with coordinates generated uniformly at random in the unit square. We compare results against the optimal solution, as different methods are hard to compare without a reference. Rather than reporting the approximation ratio $\frac{c}{c^*}$ we report the average⁸ *optimality gap* $\frac{c-c^*}{c^*} = \frac{c}{c^*} - 1$. We obtain optimal

⁷Our code in PyTorch (Paszke et al., 2017) is available on <https://github.com/wouterkool/attention-tsp>.

⁸We compute the average optimality gap using the ratio of averages of the model and optimal solutions: $\frac{\frac{1}{m} \sum_{i=1}^m c_i}{\frac{1}{m} \sum_{i=1}^m c_i^*} - 1$.

Table 1. Results of our method using greedy decoding, compared against baselines and related work. Result of Christofides’ algorithm indicated with * are reported by (Bello et al., 2016). Results of Dai et al. (2017), indicated with **, are for 15-20, 40-50 and 50-100 node graphs.

METHOD / PROBLEM	TSP20	TSP50	TSP100
OPTIMAL	3.83	5.69	7.76
NEAREST INSERTION	4.33 (12.98%)	6.78 (19.13%)	9.46 (21.80%)
RANDOM INSERTION	4.00 (4.38%)	6.13 (7.71%)	8.51 (9.65%)
FARTHEST INSERTION	3.92 (2.36%)	6.00 (5.52%)	8.35 (7.59%)
NEAREST NEIGHBOR	4.50 (17.47%)	6.98 (22.75%)	9.70 (24.98%)
CHRISTOFIDES*	4.30 (12.21%)	6.62 (16.37%)	9.18 (18.23%)
VINYALS ET AL. (2015b)	3.88 (1.25%)	7.66 (34.65%)	-
BELLO ET AL. (2016)	3.89 (1.51%)	5.95 (4.59%)	8.30 (6.89%)
DAI ET AL. (2017)**	3.89 (1.47%)	5.99 (5.33%)	8.31 (7.01%)
NOWAK ET AL. (2017)	3.93 (2.7%)	-	-
TSP20	3.84 (0.33%)	5.95 (4.60%)	9.00 (15.94%)
TSP50	3.90 (1.75%)	5.82 (2.28%)	8.23 (5.96%)
TSP100	4.17 (8.91%)	5.98 (5.13%)	8.19 (5.49%)

solutions for each instance using a MIP formulation with lazy subtour elimination constraints⁹ that we solve using Gurobi software (Gurobi Optimization, 2016).

6. Results

We indicate our models trained with different n with TSP20, TSP50 and TSP100. Since an algorithm that considers multiple solutions is incomparable to an algorithm that constructs a single solution, we compare results using greedy decoding to other learned algorithms and general baselines that also construct a single solution, and compare sampling to other methods and baselines that also sample or perform search. For details on baseline implementations, see Appendix A.

6.1. Greedy Decoding

We present our results in Table 6.1. For our models, we also report generalization performance on different n than each model was trained for, whereas for other work we only report the results for different train = test sizes n in a single row. For a better view, we plot the results in Figure 4. The vertical marker bars correspond to the columns in Table 6.1 and indicate the problem sizes that we have trained models for.

We make a number of observations. First of all, our learned algorithms improve over the best reported results of prior work significantly for all three problem sizes (when tested on the problem size trained for) and also outperform the general baselines. Second of all, we note that the model generalizes when testing on problems of different size than was trained on. Quality degrades as the difference becomes bigger, as there is *no free lunch* (Wolpert & Macready, 1997).

⁹<http://examples.gurobi.com/traveling-salesman-problem/>

Table 2. Best results of our method by sampling 1280 solutions, compared against baselines using search and sampling by Bello et al. (2016). The results marked with * and ** are reported by Bello et al. (2016) and Vinyals et al. (2015b) respectively.

METHOD / PROBLEM	TSP20	TSP50	TSP100
OPTIMAL	3.83	5.69	7.76
OR TOOLS LOCAL SEARCH*	3.85 (0.46%)	5.80 (1.95%)	7.99 (2.90%)
CHRISTOFIDES + 2OPT**	3.85 (0.46%)	5.79 (1.78%)	-
BELLO ET AL. (2016)	-	5.73 (0.72%)	8.00 (3.03%)
TSP20/50/100	3.83 (0.02%)	5.72 (0.54%)	7.97 (2.65%)
SOFTMAX TEMPERATURE	2.0	2.2	1.5

However, the results indicate that the models are able to specialize to problem sizes they are trained for.

We can make a very strong overall algorithm by selecting the trained model that works best for each instance size n (as marked in Figure 4 by the red bar). The best model does not have to be the one trained on closest matching n , but it can be determined *at train time*¹⁰ using a validation set. Testing on $n = 100$, the model trained with $n = 100$ is marginally better than the model trained with $n = 50$, but generalizes significantly better for $n > 100$. We think that for $n = 100$, the performance can be improved, for instance by pre-training on smaller sizes or using local neighborhood graphs.

6.2. Sampling

In order to compare our results to Bello et al. (2016), we use the same softmax temperature parameters¹¹ when sampling using our policy (see Appendix B for details). Table 6.2 shows the results when sampling 1280 solutions, which we consider a fair value as they can be sampled within 1 second on a single GPU for the largest instance ($n = 100$).¹² We note that we improve on the baselines and the results of Bello et al. (2016), although the difference between the models is diluted by the sampling process.

6.3. Rollout vs. other baselines

We show the benefit of our rollout baseline by evaluating the training progress. Figure 5 shows the performance of our TSP20 model at every epoch during training on a validation set using greedy decoding, compared to an exponential and a critic. We did not observe difference between using the exponential baseline and the critic, which may be the

¹⁰This is more efficient than using a paradigm such as ensembling where the best model is only known after it is evaluated at test time.

¹¹2.0, 2.2 and 1.5 for TSP20, TSP50 and TSP100.

¹²Actually we can make the sampling much more efficient as we need to encode each instance only once, which we did not do in our simple implementation.

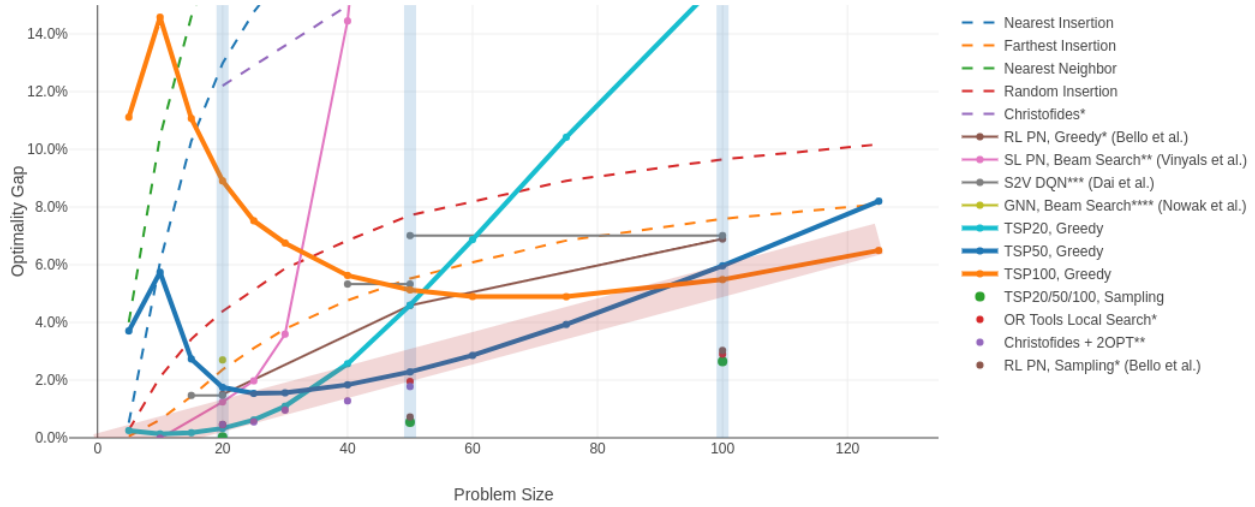


Figure 4. Optimality gap of different methods as a function of problem size $n \in \{5, 10, 15, 20, 25, 30, 40, 50, 75, 100, 125\}$. General baselines are drawn using dashed lines while learned algorithms are drawn with a solid line. Algorithms (general and learned) that perform search are plotted without connecting lines for clarity. The *, **, ***, and **** indicate that values are reported from Bello et al. (2016), Vinyals et al. (2015b), Dai et al. (2017) and Nowak et al. (2017) respectively. Best viewed in color.

7. Discussion

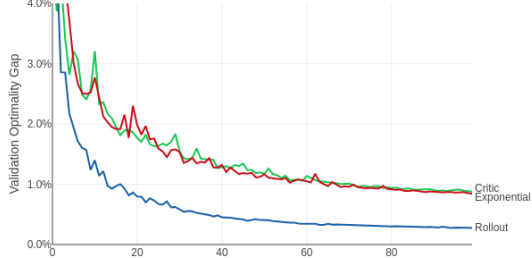


Figure 5. Held-out validation set optimality gap as a function of the number of epochs.

result of our hyperparameters¹³, but we observe significant improvements in convergence speed and quality of final results using our rollout baseline. On the x-axis we report the number of epochs such that the result looks slightly different when comparing time. The exponential baseline is faster to compute, while we found for TSP20 using a critic takes time similar to the rollout (we did not test the larger models). Still, the rollout baseline results in significantly improved speed of convergence and quality of the final results.

¹³The critic network architecture uses 3 attention layers similar to our encoder, after which the node embeddings are averaged and processed by an MLP with one hidden layer with 128 neurons and ReLu activation and a single output. We used 10^{-3} as learnrate. For the exponential baseline we used $\beta = 0.8$.

In this work we have introduced a model entirely based on attention layers and have shown that this model is capable of learning strong algorithms for the TSP, learning specialized algorithms for different problem sizes. We believe that this model is a powerful starting point for further research on learning algorithms in the context of combinatorial optimization, as it can be readily applied to general graphs.

Additionally we have shown that using a deterministic rollout of a frozen policy as a baseline in REINFORCE updates significantly improves speed of convergence and quality of final results. Combined, our model and training method resulted in state-of-the-art performance on learning algorithms for the TSP problem.

We want to emphasize that we do not claim that the method presented here is a currently a feasible alternative to state-of-the-art (non-learned) mathematical programming techniques such as implemented in Concorde (Applegate et al., 2006) and Gurobi (Gurobi Optimization, 2016), which are highly optimized and can solve TSP instances larger than we considered here to optimality. We interpret our results as evidence that there is structure in combinatorial optimization problems that can effectively be learned and used to find solutions to unseen problem instances. We plan to work on generalizing these results to problems of higher complexity, especially those of which the solution is not representable as a sequence.

Acknowledgements

This research was funded by ORTEC Optimization Technology. The authors would like to thank Thomas Kipf for helpful discussions.

References

Applegate, David, Bixby, Robert, Chvatal, Vasek, and Cook, William. Concorde tsp solver, 2006. URL <http://www.math.uwaterloo.ca/tsp/concorde/m>.

Bello, Irwan, Pham, Hieu, Le, Quoc V, Norouzi, Mohammad, and Bengio, Samy. Neural combinatorial optimization with reinforcement learning. *arXiv preprint arXiv:1611.09940*, 2016.

Dai, Hanjun, Khalil, Elias B, Zhang, Yuyu, Dilkina, Bistra, and Song, Le. Learning combinatorial optimization algorithms over graphs. *arXiv preprint arXiv:1704.01665*, 2017.

Garey, Michael R and Johnson, David S. Computers and intractability: A guide to the theory of np-completeness (series of books in the mathematical sciences), ed. *Computers and Intractability*, pp. 340, 1979.

Gurobi Optimization, Inc. Gurobi optimizer reference manual, 2016. URL <http://www.gurobi.com>.

He, Kaiming, Zhang, Xiangyu, Ren, Shaoqing, and Sun, Jian. Deep residual learning for image recognition. In *Proceedings of the IEEE conference on computer vision and pattern recognition*, pp. 770–778, 2016.

Hopfield, John J and Tank, David W. neural computation of decisions in optimization problems. *Biological cybernetics*, 52(3):141–152, 1985.

Ioffe, Sergey and Szegedy, Christian. Batch normalization: Accelerating deep network training by reducing internal covariate shift. In *International conference on machine learning*, pp. 448–456, 2015.

Kingma, Diederik P and Ba, Jimmy. Adam: A method for stochastic optimization. *arXiv preprint arXiv:1412.6980*, 2014.

LeCun, Yann, Bengio, Yoshua, and Hinton, Geoffrey. Deep learning. *nature*, 521(7553):436, 2015.

Mnih, Volodymyr, Kavukcuoglu, Koray, Silver, David, Rusu, Andrei A, Veness, Joel, Bellemare, Marc G, Graves, Alex, Riedmiller, Martin, Fidjeland, Andreas K, Ostrovski, Georg, et al. Human-level control through deep reinforcement learning. *Nature*, 518(7540):529, 2015.

Nowak, Alex, Villar, Soledad, Bandeira, Afonso S, and Bruna, Joan. A note on learning algorithms for quadratic assignment with graph neural networks. *arXiv preprint arXiv:1706.07450*, 2017.

Paszke, Adam, Gross, Sam, Chintala, Soumith, Chanan, Gregory, Yang, Edward, DeVito, Zachary, Lin, Zeming, Desmaison, Alban, Antiga, Luca, and Lerer, Adam. Automatic differentiation in pytorch. 2017.

Rosenkrantz, Daniel J, Stearns, Richard E, and Lewis, Philip M. An analysis of several heuristics for the traveling salesman problem. In *Fundamental Problems in Computing*, pp. 45–69. Springer, 2009.

Silver, David, Schrittwieser, Julian, Simonyan, Karen, Antonoglou, Ioannis, Huang, Aja, Guez, Arthur, Hubert, Thomas, Baker, Lucas, Lai, Matthew, Bolton, Adrian, et al. Mastering the game of go without human knowledge. *Nature*, 550(7676):354, 2017.

Smith, Kate A. Neural networks for combinatorial optimization: a review of more than a decade of research. *INFORMS Journal on Computing*, 11(1):15–34, 1999.

Vaswani, Ashish, Shazeer, Noam, Parmar, Niki, Uszkoreit, Jakob, Jones, Llion, Gomez, Aidan N, Kaiser, Lukasz, and Polosukhin, Illia. Attention is all you need. *arXiv preprint arXiv:1706.03762*, 2017.

Veličković, Petar, Cucurull, Guillem, Casanova, Arantxa, Romero, Adriana, Liò, Pietro, and Bengio, Yoshua. Graph attention networks. *arXiv preprint arXiv:1710.10903*, 2017.

Vinyals, Oriol, Bengio, Samy, and Kudlur, Manjunath. Order matters: Sequence to sequence for sets. *arXiv preprint arXiv:1511.06391*, 2015a.

Vinyals, Oriol, Fortunato, Meire, and Jaitly, Navdeep. Pointer networks. In *Advances in Neural Information Processing Systems*, pp. 2692–2700, 2015b.

Williams, Ronald J. Simple statistical gradient-following algorithms for connectionist reinforcement learning. *Machine learning*, 8(3-4):229–256, 1992.

Wolpert, David H and Macready, William G. No free lunch theorems for optimization. *IEEE transactions on evolutionary computation*, 1(1):67–82, 1997.

A. Details of baselines

This section describes details of the heuristics implemented for the TSP. All of the heuristics construct a single tour in a single pass, by extending a partial solution one node at the time.

A.1. Nearest neighbor

The nearest neighbor heuristic represents the partial solution as a *path* with a *start* and *end* node. The initial path is formed by a single node, selected randomly, which becomes the start node but also the end node of the initial path. In each iteration, the next node is selected as the node nearest to the end node of the partial path. This node is added to the path and becomes the new end node. Finally, after all nodes are added this way, the end node is connected with the start node to form a tour. In our implementation, for deterministic results we always start with the first node in the input, which can be considered random as the instances are generated randomly.

A.2. Farthest/nearest/random insertion

The insertion heuristics represent a partial solution as a *tour*, and extends it by *inserting* nodes one node at the time. In our implementation, we always insert the node using the *cheapest* insertion cost. This means that when node i is inserted, the place of insertion (between adjacent nodes j and k in the tour) is selected such that it minimizes the *insertion costs* $d_{ji} + d_{ik} - d_{jk}$, where d_{ji} , d_{ik} and d_{jk} represent the distances from node j to i , i to k and j to k , respectively.

The variants of the insertion heuristic vary in the way in which the node to insert is selected. Denote with S the set of nodes in the partial tour. *Nearest* insertion then inserts the node i that is nearest to (any node in) the tour:

$$i^* = \arg \min_{i \in S} \min_{j \notin S} d_{ij}. \quad (21)$$

Farthest insertion inserts the node i such that the distance to the tour (i.e. the distance from i to the nearest node j in the tour) is maximized:

$$i^* = \arg \max_{i \in S} \min_{j \notin S} d_{ij}. \quad (22)$$

Random insertion inserts a random node. Similar to nearest neighbor, we consider the input order random so we simply insert the nodes in this order.

B. Softmax temperature

When sampling a solution, we control the amount of exploration by adding a temperature parameter T to the softmax in Equation (17):

$$p_i = p_{\theta}(\pi_t = i | s, \pi_{1:t-1}) = \frac{e^{\frac{u(c)_i}{T}}}{\sum_j e^{\frac{u(c)_j}{T}}}. \quad (23)$$

Figure 6 shows how the sampling result is affected by the number of solutions sampled and the softmax temperature, for TSP50. A temperature of 0 (left in the figure) corresponds to the greedy solution. We note that with a high temperature and few solutions quality degrades (red area) as we are likely to sample suboptimal solutions. As we increase the number of solutions, we can benefit from increased temperature (up to a value indicated by the black line) because of additional exploration. Practically, this means that it is important that the temperature is selected (at train time, by evaluation) based on the number of solutions planned to generate at test time.

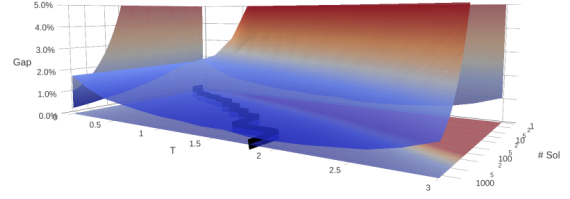


Figure 6. Optimality gap of the best solution as a function of the number of solutions sampled and softmax temperature. Note the log scale on the number of solutions axis. The line on the bottom surface indicates the optimal temperature as a function of the number of solutions sampled.